Curvature Dependence of Viral Protein Structures on Encapsidated Nanoemulsion Droplets

Connie B. Chang,[†] Charles M. Knobler,[†] William M. Gelbart,[†,‡] and Thomas G. Mason[†,‡,§,*]

[†]Department of Chemistry and Biochemistry, [‡]California NanoSystems Institute, and [§]Department of Physics and Astronomy, University of California—Los Angeles, Los Angeles, California 90095

ABSTRACT Virus-like particles are biomimetic delivery vehicles that cloak nanoscale cores inside coatings of viral capsid proteins, offering the potential for protecting their contents and targeting them to particular tissues and cells. To date, encapsidation has been demonstrated only for a relatively limited variety of core materials, such as compressible polymers and facetted nanocrystals, over a narrow range of cores sizes and of pH and ionic strength. Here, we encapsidate spherical nanodroplets of incompressible oil stabilized by adsorbed anionic surfactant using cationic capsid protein purified from cowpea chlorotic mottle virus. By imaging with transmission electron microscopy we show that, as the droplets become larger than the wild-type RNA core, the protein is forced to self-assemble into spherical shells that are not perfect icosahedra having special triangulation numbers characteristic of the Caspar—Klug hierarchy. Consequently, the distribution of protein conformations on larger droplets is significantly different than in the wild-type shell.

KEYWORDS: virus · capsid · curvature · nanoemulsion · droplet · protein · self-assembly

Pure viral capsid protein can be self-assembled around nanoscale objects,[1–3] enclosing them in protein shells through a process known as "encapsidation".[4–7] By displaying viral protein, encapsidated nanomaterials can potentially be endowed with a desirable viral functionality: preferential localization in specific tissues that could be useful for cell targeting.[8] In a classic demonstration of encapsidation, an infectious virus has been assembled *in vitro* by combining pure capsid protein with pure RNA and dialyzing to change pH and ionic strength.[1] Likewise, synthetic polymers,[9] parapolyoxometalate particles,[5] solid gold nanocrystals,[7,10,11] and quantum dots[12] have been encapsidated to create virus-like particles (VLPs)[11] similar in size to the native virus. For such small VLPs, electron microscopy indicates that the protein shell assembles from individual subunits—in a manner reminiscent of micelle formation[13]—into ordered structures[11] characteristic of icosahedral viruses,[14] including protruding ring-like multimers, or "capsomers", that have five-fold and six-fold symmetry.[15] Many water-soluble anionic polymers, including single-stranded (ss) RNA, the most prevalent viral genome, have short persistence lengths of a few nanometers, so they are compressible. Compressibility of the core permits capsid proteins to adopt specific conformations and curvatures necessary for forming highly symmetric icosahedral shells that completely envelop the polyanions.

Here, we report the encapsidation of incompressible spherical nanodroplets, or "nanoemulsions",[16] that have a continuous range of sizes extending significantly beyond the wild-type core and are stabilized by adsorbed anionic surfactant molecules. We show that it is possible to induce the capsid protein to self-assemble into spherical shells without the perfect symmetry and discrete sizes of ideal icosahedra dictated by the Caspar—Klug hierarchy,[14] which requires special integral multiples (*e.g.*, 1, 3, 4, 7, ...) of 60 proteins. Silicone oil [poly(dimethylsiloxane), PDMS]-in-water nanoemulsions stabilized by sodium dodecyl sulfate (SDS) are made by high-pressure homogenization,[17] mixed with pure cowpea chlorotic mottle virus (CCMV) capsid protein,[18] and dialyzed to reduce the divalent cation concentration, causing the protein to self-assemble.[19] Over a wide range of pH and ionic strength, the reassembly creates virus-like droplets (VLDs) coated by a single protein shell. We also explore a broad range of pH and ionic strength to control the number of concentric shells formed by the capsid protein around the nanodroplets. In the limit of low pH and ionic strength, where empty multishell structures have been formed,[20] droplets can be encapsidated inside two or more protein shells.

For VLDs coated by single shells, transmission electron microscopy (TEM) reveals that the protein has self-assembled on the

*Address correspondence to mason@chem.ucla.edu.

Received for review November 23, 2007 and accepted January 15, 2008.

Published online February 2, 2008.
10.1021/nn700385z CCC: $40.75

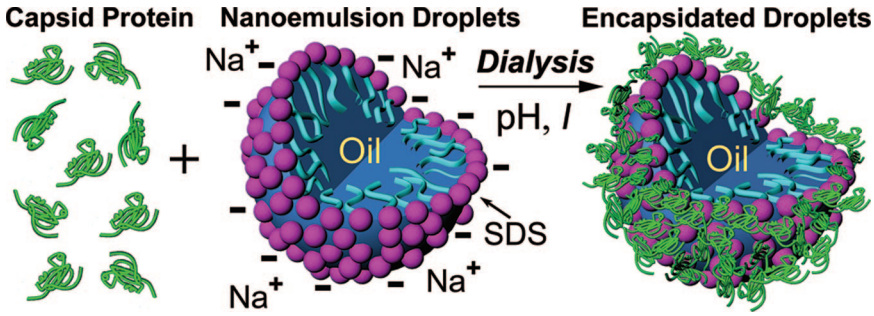

Figure 1. Schematic showing the encapsidation of an oil droplet stabilized by anionic sodium dodecyl sulfate (SDS) surfactant in water by purified capsid protein from cowpea chlorotic mottle virus (CCMV). By adjusting the pH and ionic strength *I* using dialysis, the capsid protein in bulk solution can be induced to condense and assemble around the negatively charged surfaces of the nanoemulsion droplets.

curved surfaces not only into ordered capsomers but also into a variety of other structures. As the droplet surface curvature is reduced, ordered capsomer structures become less prevalent, and other protein structures appear: defected capsomers, hexagonal webs, and trough-like scars. Some of these structures appear to be due to jamming[21] of the protein on the curved surface and are reminiscent of defects found on macroscopic droplets stabilized by solid microscopic particles.[22–24] However, other structures, such as the hexagonal web, arise from special rules associated with attractive protein–protein and protein−surface interactions. The overall reduction in the population of ordered capsomers on larger droplets implies that the three different conformations of the protein[25] in the capsid of CCMV are not present in the same proportions when the protein assembles on incompressible surfaces that have lower curvature. Thus, surface curvature plays an essential role in setting protein conformation and profoundly influences the structure of assembled proteins that encapsidate incompressible objects.

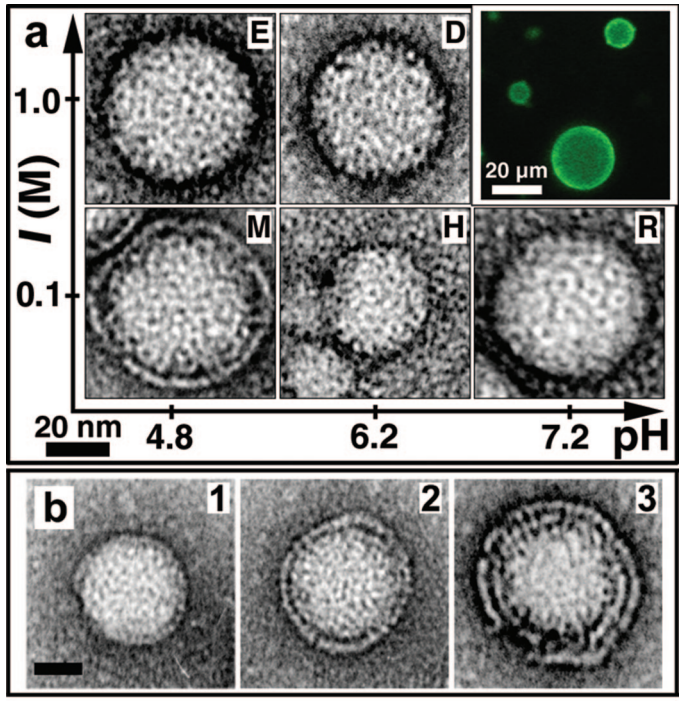

Figure 2. Capsid protein structures observed by negatively stained TEM. (a) Individual nanoscale droplets as a function of pH and ionic strength *I* of NaCl after mixing and dialyzing SDS-stabilized nanoemulsions with purified CCMV protein. Buffers are defined as follows: RNA-reassembly, R (pH = 7.2, *I* = 0.1 M); hexagonal sheet, H (pH = 6.2, *I* = 0.1 M); dimer, D (pH = 6.2, *I* = 1.0 M); multi-shell, M (pH = 4.8, *I* = 0.1 M); and empty shell, E (pH = 4.8, *I* = 1.0 M). Inset (upper right): Fluorescence optical micrograph of FITC-labeled CCMV protein (green) covering the surfaces of microscale silicone oil droplets stabilized by SDS after dialysis with R buffer. (b) Nanodroplets encapsidated by one, two, and three concentric protein shells are observed after dialysis with M buffer. Scale bar = 20 nm (all images).

RESULTS AND DISCUSSION

Anionically stabilized nanodroplets provide incompressible, charged templates that offer a wide range of curvatures upon which capsid protein can be assembled. Through extreme emulsification,[16] we make oil-in-water nanoemulsions comprised of spherical droplets that can be as small as CCMV (inner diameter of 21 nm and outer diameter of 28 nm). Relying upon differences in creaming rates, ultracentrifugal size-fractionation provides uniform model nanoemulsions having droplet radii between 10 nm $< a <$ 100 nm.[17] In addition, the droplet volume fraction φ and surfactant concentration C_{SDS} can be set independently. The Laplace pressure, corresponding to the stress necessary to overcome surface tension and deform a droplet, is typically above 10 atm, so droplets are spherical at dilute φ. To inhibit Ostwald ripening,[26] which can lead to unwanted growth of the droplets through molecular diffusion, the dispersed liquid is chosen to be very insoluble in the continuous liquid phase.

We create VLDs by mixing pure, disassembled CCMV capsid protein with an oil-in-water nanoemulsion and changing the pH and NaCl ionic strength, *I*, of the buffer through dialysis, causing the protein to assemble on the droplet surfaces (see Figure 1). TEM of negatively stained VLDs reveals the presence of ordered protein structures, including ring-like capsomers, on the surfaces of individual droplets. To probe a diversity of structures, we have encapsidated SDS-coated nanodroplets at five different buffer conditions, corresponding to the known phase behavior of the protein:[2,20,27] RNA-reassembly (pH = 7.2, *I* = 0.1 M), hexagonal sheet (pH = 6.2, *I* = 0.1 M), dimer (pH = 6.2, *I* = 1.0 M), multishell (pH = 4.8, *I* = 0.1 M), and empty shell (pH = 4.8, *I* = 1.0 M). We show TEM images of negatively stained VLDs for these buffers in Figure 2a. Protein-coated nanodroplets can be distinguished from empty capsid shells because the uranyl acetate staining does not penetrate into the core of the coated droplets, so they appear noticeably brighter in the center. A darker ring

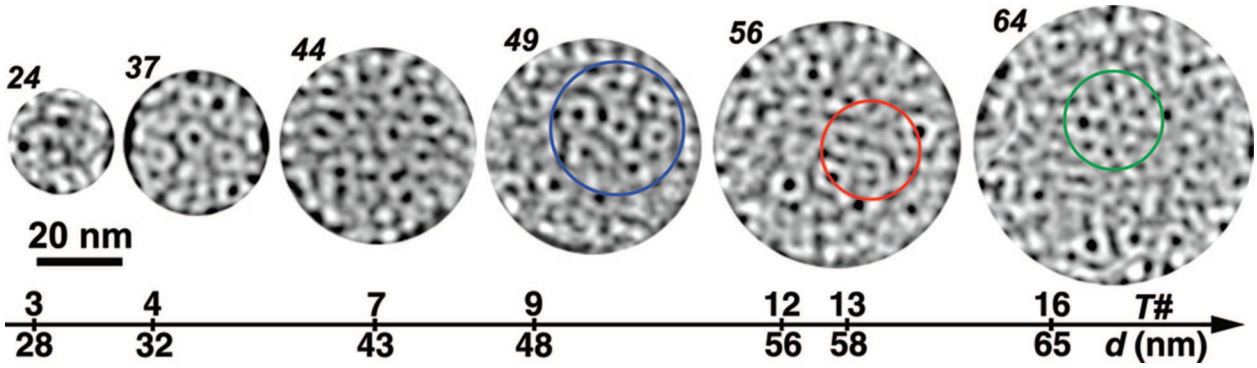

Figure 3. Representative examples of CCMV protein structures observed as a function of the droplet diameter, *d* (italic numbers), on a single side of individual encapsidated oil nanodroplets after dialysis using RNA-reassembly buffer. TEM images have been background subtracted and Fourier filtered to enhance the protein structures on the droplet surfaces. Complete protein "capsomers" (white rings) are found more often on the surfaces of smaller nanodroplets that have sizes closer to that of the native virus. Ring-like capsomers can order into six-fold arrangements locally (blue circle). Extended dark trough-like "scars" (red circle), defected capsomers, and hexagonal web-like networks of capsid protein (green circle) are more frequently seen on larger droplets. Allowed triangulation numbers *T* and predicted outer diameters of nanodroplets that could be encapsidated by perfect icosahedra of ordered capsomers are shown in the lower scale. The outer diameters (in nm) are estimated using[32] $d(T) \approx 28(T/3)^{1/2}$, consistent with $d = 28$ nm for CCMV, a $T = 3$ virus.

around the edges of the droplets exists due to the trapping of the stain as the water contact line recedes during the evaporation process. This staining and drying process yields TEM images that provide excellent views of only one half of the surface of each droplet. Because the images do not contain a significant signal from the protein on the other half, it is possible to identify and interpret the protein surface structure on *individual* droplets, rather than having to rely on reconstruction methods that presume an ordered structure.

For all five buffers, CCMV protein encapsidates nanodroplets, regardless of their size (Figure 2a). Dimer buffer and RNA-reassembly buffer create VLDs efficiently without any loss of protein into empty shells. For the multi-shell buffer, we observe nanodroplets coated with single, double (dominant), and triple shells (Figure 2b). For the empty-shell and multi-shell buffer conditions, due to the slight excess of protein beyond that required to coat the droplets, we observe encapsidated droplets and also empty shells.

To confirm that the protein is not simply deposited on the droplet surfaces during drying but actually assembles around the droplets while in solution, we have examined fluorescein isothiocyanate (FITC)-labeled CCMV protein on microscale silicone oil droplets after dialyzing with RNA-assembly buffer. Strong fluorescence emanates from the surfaces of the droplets (Figure 2a inset), indicating that they are coated with the labeled protein. By contrast, when droplets coated with cationic cetyl trimethylammonium bromide (CTAB) surfactant are mixed with FITC-labeled CCMV proteins and dialyzed in the same manner, no surface fluorescence is observed.

We have also examined the structures and relative degree of order and disorder of protein on nanodroplets having different curvatures for RNA-reassembly conditions (Figure 3). To enhance the images of the structures on the surfaces of individual VLDs, we remove the background and then reduce high-frequency noise using Fourier filtering. We identify complete capsomers as white rings that have an internal dark central spot and also a dark external trough surrounding the bright ring. The brighter regions indicate a higher density of proteins that project outward from the surfaces, and the darker regions generally indicate a lower density of protein where stain becomes more highly concentrated in the local depressions. As the droplets become progressively larger than CCMV, complete capsomers become less prevalent, and several other protein structures are observed on the less curved incompressible surfaces. In particular, imperfect capsomers, linear scar-like defects, and hexagonal web-like structures are seen, in sharp contrast to perfect icosahedral order on wild-type CCMV. Based on energy minimization, a greater relative coverage of the droplets by ordered capsomers might be expected when droplet sizes correspond to allowed integral triangulation numbers *T* [14,28] (see Figure 3, lower scale), yet this assumes that the structure and size of the capsomers will not be influenced by the underlying curvature and degree of compressibility of the core. Although our experiments at all buffer conditions do not reveal a higher degree of capsomer order on droplets that correspond to allowed *T*, this might occur at different pH and *I* than we have yet explored.

For smaller droplets closer to the size of the native virus, we have identified local hexagonal packing of capsomers (Figure 4a, left), as can be seen on the native virus. Although we find numerous examples of six capsomers surrounding a central capsomer, five-fold-coordinated capsomers without defects have not been observed on droplets significantly larger than CCMV. The distribution of center-to-center distances between neighboring six-fold capsomers is shown in Figure 4b, and the average distance of 9.5 nm is in excellent agreement with that known from native CCMV.[25]

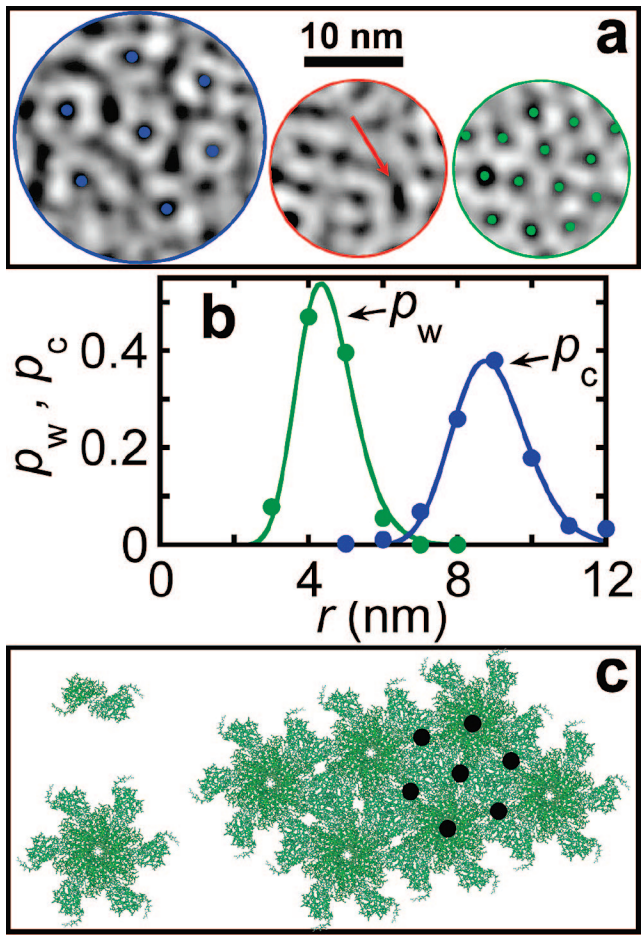

Figure 4. Local protein structures observed on the surfaces of nanodroplets (enlarged from colored circles in Figure 3) have different degrees of order and disorder. (a) Left: six-fold-coordinated capsomers (blue dots at center) represent a high degree of order seen mostly on smaller droplets. Middle: an example of a trough-like scar that consists of an elongated dark region (red arrow) surrounded by a protruding white region. Right: hexagonal web structure, typically seen on larger droplets, consisting of dark spots (green dots) surrounded by an interconnected white network of protein protruding from the interface. (b) Probabilities p_c and p_w *versus* distance, *r*, between centers of dark regions for hexagonal capsomers and web, respectively. The average spacing between the dark spots of the web (4.7 nm) is roughly half of the distance between the centers of capsomers (9.5 nm). (c) A web-like structure (right) can be made by packing hexagonal capsomers (lower left) of hand-in-glove protein dimers[25] (upper left) on a flat surface. Regions of low protein density are marked in one hexagonal cell with black dots.

On a number of larger droplets, we observe a hexagonal web-like structure of protein: regions of dark dots surrounded by interconnected white boundaries, or "web" (Figure 4a, right). Dark outer troughs characteristic of capsomers are absent. Although this protein web usually has local six-fold hexagonal order, in general, it can be disordered due to defects. The average distance between nearest-neighbor dots in the web is only 4.7 nm, about half the distance between the centers of capsomers (Figure 4b). This is consistent with capsid protein self-assembling in a different manner on flatter, incompressible surfaces than on more highly curved, compressible surfaces.[2]

We propose that the mechanism of the formation of the hexagonal web structure of protein can be understood by considering the underlying symmetry and dense packing of self-assembled protein subunits on incompressible surfaces of lower curvature. CCMV capsid protein is known to self-assemble into hexagonal capsomers of hand-in-glove dimers[20,29] that have been identified by X-ray cystallography. These dimers are energetically favored over monomers in many buffer conditions; a protruding arm of one protein is inserted into the folded region of its partner and is held by an attraction, and *vice versa*.[30] Six hand-in-glove dimers can join together to form a capsomer that has six protruding arms in a structure resembling a gear (Figure 4c, lower left). Such capsomer structures are also energetically favored over a random assembly of dimers. When these gear-like hexagonal capsomers of dimers self-assemble and then densely pack to cover a flat surface, they can create hexagonal arrays of capsomers that have regions that are depleted of protein at half of the center-to-center distance between neighboring capsomers. This packed-gear structure would give the appearance of the web that we observe: a hexagonal array of dark spots where the protein density is lower, and an interconnected hexagonal network of bright web where the protein density is higher. For self-assembly of protein on a flat surface, it is reasonable to assume that the folded capsid protein and dimers exist in only a single conformation and do not distort into the three known conformations that are required for assembling five-fold-coordinated capsomers on core structures that have higher curvature comparable to that of the wild-type virus.

In addition to the ordered web, we also observe elongated protein scars that are dark troughs surrounded by white rims (Figure 4a, middle). These protein scars bear some resemblance to scar defects found in the packing of monodisperse solid spheres on the surfaces of curved liquid droplets,[22,23] a controlled variety of "Pickering emulsions",[24,30,31] yet capsid protein scars are distinctly different. Protein scars do not consist simply of line defects between fully formed hexagonal ring-like capsomers on incommensurately sized droplets; instead they indicate disorder of the protein at a smaller scale than even the capsomer unit itself. Several mechanisms combine to produce the scar defects: incommensurate sizes of the droplets relative to those corresponding to allowed *T* numbers for icosahedral structures, and surface jamming of the protein that strongly inhibits protein reorientation and rearrangement once the surface is completely covered.

CONCLUSIONS

A variety of protein structures, including dimers, partial capsomers, and complete capsomers, may become jammed into locally disordered states[21] on incompress-

ible spherical surfaces that have reduced curvature in a manner reminiscent of out-of-equilibrium glasses and gels. Additional defects may arise because protein adsorbed at high densities may not be able to change conformation and reorganize into lowest-energy ordered states, as when forming around RNA. Controlling the relative protein coverage and examining the kinetics of the process of encapsidation will provide greater insight into how ordered and disordered protein structures arise on the surfaces of VLDs. By adjusting the pH and ionic strength, it may be possible to encapsidate droplets, nanoparticles, and synthetic polymers with a controlled number of capsid shells.

By interpreting TEM images of individual encapsidated nanodroplets, we have revealed a range of novel structures, including defected capsomers, hexagonal web, and scars, on the surfaces of the droplets. The discovery of these structures provides significant new insight into the nature of protein conformations on curved surfaces. Moreover, our observations show that non-equilibrium protein structures can exist on encapsidated nanoscale objects due to surface jamming on an incompressible charged template. Thus, the picture of thermodynamic self-assembly of perfect icosahedral shells around artificial nanostructures may be correct only in certain limiting cases.

METHODS

Protein Purification. Following Choi and Rao's procedure,[18] we isolate and purify capsid protein from CCMV. Purified CCMV is dialyzed for 24 h in 1.0 L of disassembly buffer (0.5 M $CaCl_2$, 50 mM Tris-HCl at pH 7.5, 1.0 mM EDTA, 1.0 mM DTT, 0.5 mM PMSF). The dissociated virus is centrifuged for 30 min at 14 000 rpm to precipitate the RNA. The protein supernatant is extracted and dialyzed for 24 h in 1.0 L of RNA-reassembly buffer (50 mM NaCl, 50 mM Tris-HCl, pH 7.2, 10 mM KCl, 5.0 mM $MgCl_2$, 1.0 mM DTT). The solution is then centrifuged for 100 min at 100 000 rpm, and the protein supernatant is extracted. The concentration and purity of the protein are measured using UV–visible spectroscopy. All work is performed at 4 °C.

Nanoemulsion Preparation and Fractionation. Nanoemulsions are created using extreme flow with a high-pressure microfluidic device.[17] Polydisperse emulsions are size-fractionated using ultracentrifugation to achieve better droplet uniformity and to set the SDS concentration C_{SDS}. Prior to mixing with protein and dialyzing, the nanoemulsions have $C_{SDS} = 1$ mM SDS, well below the critical micelle concentration, and $\varphi = 0.05$. The PDMS oil (10 cSt viscosity, supplied by Gelest) has a low vapor pressure, so it does not evaporate over the time scale of our microscopy measurements, even when capsid protein is not present.

Dialysis Buffers. The composition of each buffer is as follows. RNA-reassembly buffer:[27] Tris-HCl buffer at pH = 7.2, $I = 0.10$ M NaCl, 10 mM KCl, 5.0 mM $MgCl_2$, and 1.0 mM DTT. Empty shell buffer: 50 mM sodium acetate buffer at pH = 4.8 and $I = 1.0$ M NaCl. Dimer buffer: 50 mM sodium phosphate buffer at pH = 6.2 and $I = 1.0$ M NaCl. Multishell buffer: 50 mM sodium acetate buffer at pH = 4.8 and $I = 0.1$ M NaCl. Hexagonal sheet buffer: 50 mM sodium phosphate buffer at pH = 6.2 and $I = 0.1$ M NaCl. The last four buffers also contain 1.0 mM EDTA and 1.0 mM DTT.

Encapsidation Procedure. A 10 μL aliquot of stock nanoemulsion at 1.0 mM SDS and $\varphi = 0.05$ is added to purified CCMV protein at 0.15 μg/mL to give a total reaction volume of 200 μL. The mixture is dialyzed in 1.0 L of the appropriate buffer for 24 h at 4 °C. The SDS concentration after dilution and dialysis is roughly 10^{-5} M, so SDS−protein binding interaction in the bulk solution is minimized while still maintaining droplet stability. The sulfate head group of SDS remains negatively charged over the entire range of pH we access. After dilution, the charge density of SDS on the oil–water interfaces is roughly -0.1 e/nm^2.

Transmission Electron Microscopy: Staining and Analysis. Pelco copper grids of 400 mesh size and 3.0 mm outer diameter (Ted Pella, Inc.) are coated with a thin film of parlodion and carbon. The grids are glow-discharged using high-voltage, alternating current immediately before sample deposition. We place 5 μL of the sample directly onto the grid for 1 min and then wick with Whatman 4 filter paper and immediately stain with a 1% solution of uranyl acetate in water for 1 min. The samples are air-dried and viewed under a Hitachi H-7000 electron microscope at an accelerating voltage of 75 kV. Negatives were developed and scanned using a Minolta Dimage Scan MultiPro scanner for image analysis. Adobe Photoshop is used to flatten the image background by subtracting a strongly blurred image. Cross-correlation Fourier-transform image analysis is applied using a correlation kernel that has a dark center, corresponding to the size of the capsomer's dark dimple and a white outer ring.

Fluorescence Microscopy. We make a stock solution of FITC in DMSO at 1.0 mg/mL. An aliquot of the FITC stock solution is added to dissociated CCMV protein and equilibrated in 50 mM phosphate buffer at pH = 8.2. The protein and dye are mixed, and, after 8 h, the FITC-labeled protein is dialyzed into RNA-reassembly buffer, lowering the pH. Next, the FITC-labeled protein solution is mixed with 10 μL of microscale emulsions at 1.0 mM concentrations of either SDS or CTAB to $\varphi = 0.05$ in a total reaction volume of 200 μL and dialyzed using RNA-reassembly buffer. Fluorescence micrographs reveal the presence of labeled protein at the droplet surfaces through strong fluorescence at the edges of the droplets. Microscale emulsions in the absence of labeled protein do not show this fluorescence. Therefore, droplets that are much larger than the native virus can be coated by a dual layer of anionic surfactant and virus protein. Irreversible protein adsorption likely inhibits the equilibrium exchange of surfactant to and from the droplet interfaces.

Acknowledgment. We thank M. Phillips for assisting with the TEM measurements, A. Levine for useful discussions, and the John McTague Chair for financial support.

Supporting Information Available: Transmission electron micrographs of reassembled CCMV capsid protein in the absence of nanodroplets, shown for a variety of buffer conditions as control experiments. This information is available free of charge *via* the Internet at http://pubs.acs.org.

REFERENCES AND NOTES

1. Bancroft, J. B.; Hiebert, E. Formation of an Infectious Nucleoprotein from Protein and Nucleic Acid Isolated from a Small Spherical Virus. *Virology* **1967**, *32*, 354–356.
2. Bancroft, J. B.; Hills, G. J.; Markham, R. A Study of the Self-Assembly Process in a Small Spherical Virus. Formation of Organized Structures from Protein Subunits *in Vitro*. *Virology* **1967**, *31*, 354–379.
3. Hiebert, E.; Bancroft, J. B.; Bracker, C. E. The Assembly *in Vitro* of Some Small Spherical Viruses, Hybrid Viruses, and Other Nucleoproteins. *Virology* **1968**, *34*, 492–508.
4. Douglas, T.; Strable, E.; Willits, D.; Aitouchen, A.; Libera, M.; Young, M. Protein Engineering of a Viral Cage for Constrained Nanomaterials Synthesis. *Adv. Mater.* **2002**, *14*, 415–418.
5. Douglas, T.; Young, M. Host-Guest Encapsulation of Materials by Assembled Virus Protein Cages. *Nature* **1998**, *393*, 152–155.
6. Douglas, T.; Young, M. Virus Particles as Templates for Materials Synthesis. *Adv. Mater.* **1999**, *11*, 679–681.

7. Dragnea, B.; Chen, C.; Kwak, E. S.; Stein, B.; Kao, C. C. Gold Nanoparticles as Spectroscopic Enhancers for *in Vitro* Studies on Single Viruses. *J. Am. Chem. Soc.* **2003**, *125*, 6374–6375.
8. Uchida, M.; Klem, M. T.; Allen, M.; Suci, P.; Flenniken, M.; Gillitzer, E.; Varpness, Z.; Liepold, L. O.; Young, M.; Douglas, T. Biological Containers: Protein Cages as Multifunctional Nanoplatforms. *Adv. Mater.* **2007**, *19*, 1025–1042.
9. Bancroft, J. B.; Hiebert, E.; Bracker, C. E. The Effects of Various Polyanions on Shell Formation of Some Spherical Viruses. *Virology* **1969**, *39*, 924–930.
10. Chen, C.; Daniel, M. C.; Quinkert, Z. T.; De, M.; Stein, B.; Bowman, V. D.; Chipman, P. R.; Rotello, V. M.; Kao, C. C.; Dragnea, B. Nanoparticle-Templated Assembly of Viral Protein Cages. *Nano Lett.* **2006**, *6*, 611–615.
11. Sun, J.; DuFort, C.; Daniel, M.-C.; Murali, A.; Chen, C.; Gopinath, K.; Stein, B.; De, M.; Rotello, V. M.; Holzenburg, A.; *et al.* Core-Controlled Polymorphism in Virus-Like Particles. *Proc. Natl. Acad. Sci. U.S.A.* **2007**, *104*, 1354–1359.
12. Dixit, S. K.; Goicochea, N. L.; Daniel, M.-C.; Murali, A.; Bronstein, L.; De, M.; Stein, B.; Rotello, V. M.; Kao, C. C.; Dragnea, B. Quantum Dot Encapsulation in Viral Capsids. *Nano Lett.* **2006**, *6*, 1993–1999.
13. McPherson, A. Micelle Formation and Crystallization as Paradigms for Virus Assembly. *BioEssays* **2005**, *27*, 447–458.
14. Zandi, R.; Reguera, D.; Bruinsma, R. F.; Gelbart, W. M.; Rudnick, J. Origin of Icosahedral Symmetry in Viruses. *Proc. Natl. Acad. Sci. U.S.A.* **2004**, *101*, 15556–15560.
15. Caspar, D. L.; Klug, A. Physical Principles in the Construction of Regular Viruses. *Cold Spring Harb. Symp. Quant. Biol.* **1962**, *27*, 1–24.
16. Mason, T. G.; Wilking, J. N.; Meleson, K.; Chang, C. B.; Graves, S. M. Nanoemulsions: Formation, Structure, and Physical Properties. *J. Phys.: Condens. Matter* **2006**, *18*, R635–R666.
17. Meleson, K.; Graves, S.; Mason, T. G. Formation of Concentrated Nanoemulsions by Extreme Shear. *Soft Mater.* **2004**, *2*, 109–123.
18. Choi, Y. G.; Rao, A. L. N. Molecular Studies on Bromovirus Capsid Protein: VII Selective Packaging of BMV RNA4 by Specific n-Terminal Arginine Residues. *Virology* **2000**, *275*, 207–217.
19. Adolph, K. W.; Butler, P. J. G. Reassembly of a Spherical Virus in Mild Conditions. *Nature* **1975**, *255*, 737–738.
20. Adolph, K. W.; Butler, P. J. Studies on the Assembly of a Spherical Plant Virus. I. States of Aggregation of the Isolated Protein. *J. Mol. Biol.* **1974**, *88*, 327–341.
21. Liu, A. J.; Nagel, S. R. Jamming Is Not Just Cool Any More. *Nature* **1998**, *396*, 21–22.
22. Bausch, A. R.; Bowick, M. J.; Cacciuto, A.; Dinsmore, A. D.; Hsu, M. F.; Nelson, D. R.; Nikolaides, M. G.; Travesset, A.; Weitz, D. A. Grain Boundary Scars and Spherical Crystallography. *Science* **2003**, *299*, 1716–1718.
23. Bowick, M.; Cacciuto, A.; Nelson, D. R.; Travesset, A. Crystalline Order on a Sphere and the Generalized Thomson Problem. *Phys. Rev. Lett.* **2002**, *89*, 1–4.
24. Tarimala, S.; Dai, L. L. Structure of Microparticles in Solid-Stabilized Emulsions. *Langmuir* **2004**, *20*, 3492–3494.
25. Speir, J. A.; Munshi, S.; Wang, G.; Baker, T. S.; Johnson, J. E. Structures of the Native and Swollen Forms of Cowpea Chlorotic Mottle Virus Determined by X-Ray Crystallography and Cryo-Electron Microscopy. *Structure* **1995**, *3*, 63–78.
26. Taylor, P. Ostwald Ripening in Emulsions: Estimation of Solution Thermodynamics of the Disperse Phase. *Adv. Colloid Interface Sci.* **2003**, *106*, 261–285.
27. Adolph, K. W.; Butler, P. J. Assembly of a Spherical Plant Virus. *Philos. Trans. R. Soc. London B* **1976**, *276*, 113–122.
28. Bruinsma, R. F.; Gelbart, W. M.; Reguera, D.; Rudnick, J.; Zandi, R. Viral Self-Assembly as a Thermodynamic Process. *Phys. Rev. Lett.* **2003**, *90*, 1–4.
29. Tang, J.; Johnson, J. M.; Dryden, K. A.; Young, M. J.; Zlotnick, A.; Johnson, J. E. The Role of Subunit Hinges and Molecular 'Switches' in the Control of Viral Capsid Polymorphism. *J. Struct. Biol.* **2006**, *154*, 59–67.
30. Pickering, S. U. Emulsions. *J. Chem. Soc. Trans. London* **1907**, *91*, 2001–2021.
31. Subramaniam, A. B.; Abkarian, M.; Stone, H. A. Controlled Assembly of Jammed Colloidal Shells on Fluid Droplets. *Nat. Mater.* **2005**, *4*, 553–556.
32. Hu, Y.; Zandi, R.; Anavitarte, A.; Knobler, C. M.; Gelbart, W. M. Packaging of a Polymer by a Viral Capsid: The Interplay between Polymer Length and Capsid Size. *Biophys. J.* **2008**, *94*, 1428–1436.